

## Phase-Field Modelling of a Multiphase Material

Hugo M. Leão<sup>1</sup>, Roque L. da S. Pitangueira<sup>1</sup>, Lapo Gori<sup>1</sup>, Ramon P. da Silva<sup>1</sup>,

<sup>1</sup>Structural Engineering Department, Federal University of Minas Gerais  
Av. Antônio Carlos, 6627, Pampulha, Belo Horizonte, 31270-901, Minas Gerais, Brazil  
hugomleao@yahoo.com.br, roque@dees.ufmg.br, lapo@dees.ufmg.br, ramon@dees.ufmg.br

**Abstract.** The Phase-Field Modelling has been widely used to model crack propagation. In that model, the discrete crack of Griffith's theory is transformed into a diffuse crack that spreads on a certain region, according to the length scale parameter. The Phase-Field variable is calculated as a new nodal degree of freedom. It represents, at each point, the amount of damage suffered by the material, in such way that when it's zero the material is intact, and when it's equal to one the material is completely damaged. In this work the Phase-Field analysis has been used to study the fracture process in a multiphase material, composed by a mortar with aggregates randomly distributed across the domain. The influence of the material properties on the structural behaviour was also investigated. All the implementation was done in INSANE, an open-source software, developed in Java at the Structural Engineering Department of the Federal University of Minas Gerais. Numerical simulations will be presented considering the variation of the sample size and the parameters of the materials.

**Keywords:** Phase-Field Modelling, Crack Propagation, Diffusive Crack, Finite Element Method, INSANE Software

### 1 Introduction

The computational numerical modelling for concrete has been approached for a long time by the scientific community [1–6]. In the last years, the Phase-Field modelling has been used as an alternative since the model easily allows the insertion of heterogeneities and can auto-detect the crack path [7–10]. Having its development started by Bourdin et al. [11], the Phase-Field approach replaces the discrete crack  $\Gamma$  proposed by Griffith for a diffuse crack that extends along a region  $\mathcal{B}$  with boundary  $\partial\mathcal{B}$  (See Fig. 1). For that a new degree of freedom

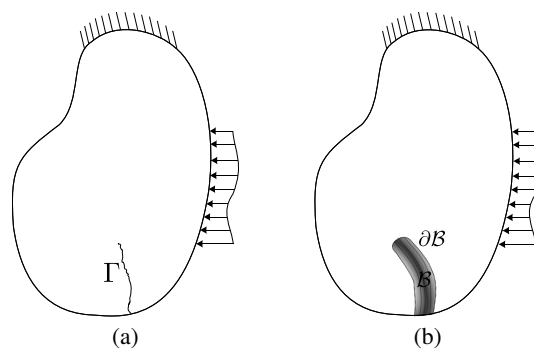


Figure 1. Comparison between (a) Griffith crack and (b) Phase-Field diffuse crack

is inserted. This additional degree of freedom varies from zero to one, and represents the damage suffered by the material in the region  $\mathcal{B}$ .

In this work, the Phase-Field modelling has been used to deal with material heterogeneities. In this way, the behaviour of a concrete specimen, composed by mortar and aggregates randomly distributed across the domain, will be presented. All the implementation was done in *INSANE*<sup>1</sup> (INteractive Structural ANalysis Environment),

<sup>1</sup>More information on the project can be found at <https://www.insane.dees.ufmg.br/> and the development code is freely

an open source software developed in Java by the Structural Engineering Department of the Federal University of Minas Gerais, and has been largely used by the research group since 2002.

## 2 Specimen Size

In order to investigate the influence of the size on the behaviour of the specimen, the 6 samples illustrated in Fig. 2 were modelled. In each one of them, the aggregates were randomly distributed up to a 30% covering of the domain. For that, the *Take and Place* method, based on Wang et al. [12] and Wriggers and Moftah [13], was used. The aggregates grading curve considered in the present analysis has Fuller exponent equal to 0.7909 with minimum and maximum sieves sizes of 4.75 and 12.5 mm, respectively.

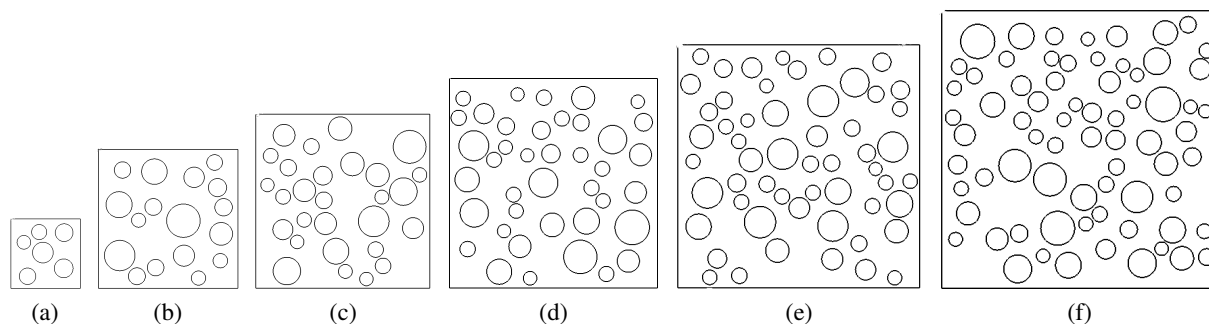


Figure 2. Aggregate distribution for sample of (a) 25 mm, (b) 50 mm, (c) 62.5 mm, (d) 75 mm, (e) 87.5 mm, (f) 100 mm.

These samples were tested considering for both the mortar and the aggregates a Phase-Field isotropic constitutive model, with no split in the strain energy, was considered. The linear energetic degradation function and the geometric crack function of Wu [14] with parameter  $\xi = 2$  were considered for both the materials. Further parameters are described in Table 1.

Table 1. Material parameters

Material	Elasticity Modulus ( $E_0$ ) [N/mm <sup>2</sup> ]	Poison's rate ( $\nu$ ) [–]	Fracture Energy ( $G_c$ ) [N/mm]	Tensile strength ( $f_t$ ) [N/mm <sup>2</sup> ]
Aggregate	100000.0	0.20	0.1300	16.0
Mortar	21876.0	0.18	0.0018	3.48

In the problem setting, the horizontal displacement of the left side was restricted, and a horizontal displacement was imposed on the right side. The analysis were performed in a plane stress state, with 1 mm of thickness. A triangular mesh with mean nodal distance of 1.5 mm was adopted across the whole domain. In both materials the length scale parameter was defined as  $l_0 = 3.0$  mm.

The obtained results were depicted in Figs. 3 and 4. It can be noted that as the sample becomes larger, the structural response is more fragile. From the phase-field contour plot it is clear that, when facing an aggregate, the crack deviates its way, seeking an alternative path that minimizes energy functional.

## 3 Mortar Properties

This section presents the behaviour of the heterogeneous composite under a traction test, modelled using Phase-Field, and varying the mortar properties. For that, the sample of 50 mm, and the material properties presented in section 2 were used. In the first subsection the influence of the fracture energy parameter was tested, in

available at the Git repository <http://git.insane.dees.ufmg.br/insane/insane.git>.

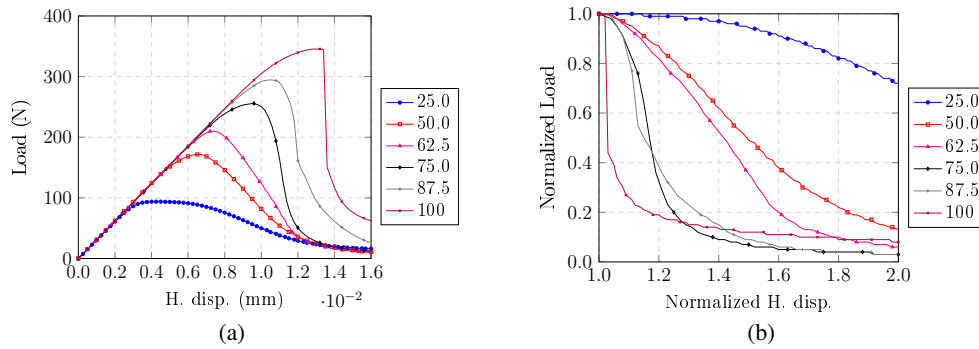


Figure 3. (a) Load-displacement curve and (b) Normalized load-displacement curve.

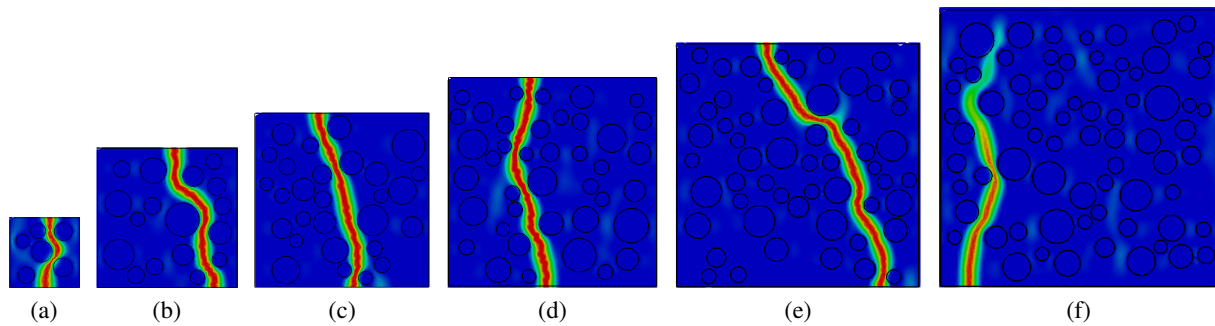


Figure 4. Phase-field contour plot for (a) 25 mm, (b) 50 mm, (c) 62.5 mm, (d) 75 mm, (e) 87.5 mm, (f) 100 mm.

the second subsection, the influence of the elasticity modulus, and in the last subsection it was analysed how the mortar tensile strength affects the final response.

### 3.1 Different Fracture Energy Parameters

The load-displacement curves obtained for various values for the fracture energy ( $G_c$ ) are illustrated in Fig. 5. The legend of the graphs indicates the considered fracture energy for each curve, and the numerical unit of the presented values are N/mm. The Phase-Field contour plot is similar to that one presented in Fig. 4.b.

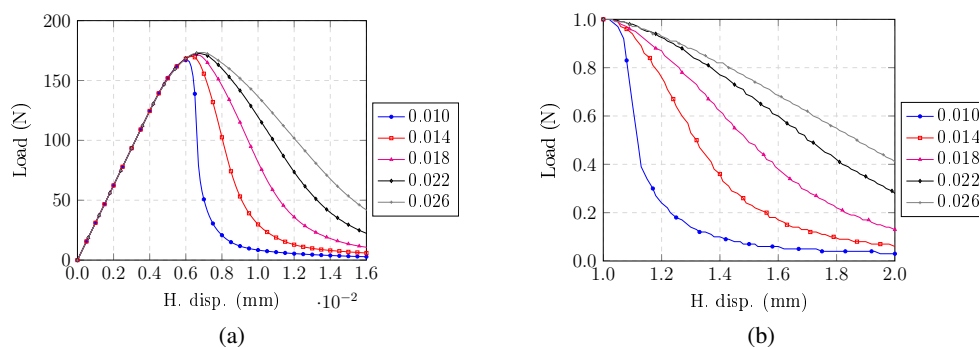


Figure 5. Load-displacement curves for various fracture energy ( $G_f$ ) parameters. The unit of the terms shown in legend is N/mm. (a) Load-displacement curve. (b) Normalized load-displacement curve.

As expected, the variation in the fracture energy parameter does not change the initial rising part of the curve, once that, as the material has not cracked yet, its behaviour remains linear elastic. When the crack starts to propagate, it can be observed that the material with higher fracture energy behaves more ductile and has a small

increasing on its maximum strength. That observed behaviour is coherent since that material with higher  $G_f$  needs to absorb more strain energy to make the crack grow.

### 3.2 Different Elasticity Modulus

The influence of the elasticity modulus parameter of mortar in the structural behaviour was also tested. Fig. 6 presents the load-displacement curves considering the same sample of previous subsection and various elasticity modulus values.

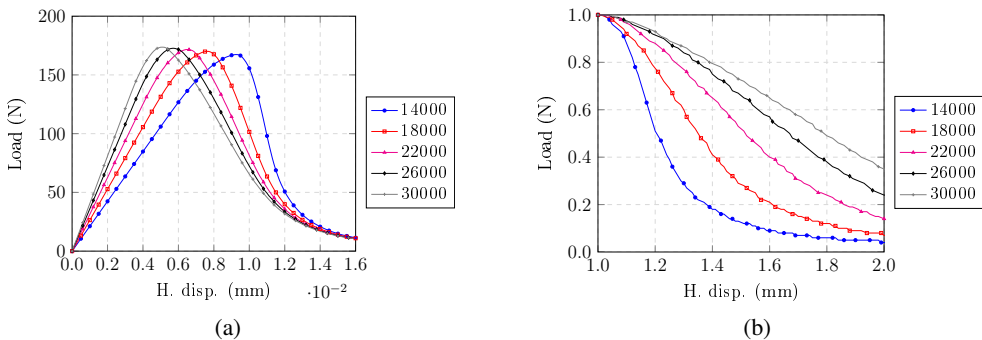


Figure 6. Load-displacement curves for various elasticity modulus ( $E_0$ ) parameters. The unit of the therms shown in legend is  $N/mm^2$ . (a) Load-displacement curve. (b) Normalized load-displacement curve.

From Fig. 6 it can be observed that the increasing of mortar  $E_0$  makes the structure behaves more ductile. The peak load remains around the same value since that property is more related to the mortar tensile strength. See next subsection, in which this test is redone varying, however, the mortar tensile strength.

### 3.3 Different Tensile Strength

In this subsection, the traction tests of the 50-mm-size sample were performed by varying the mortar tensile strength considering the following values:  $f_t = 2.5, 3.0, 3.5, 4.0$  and  $4.5 N/mm^2$ . Fig. 7 shows the load-displacement and the normalized load-displacement curves for each considered parameter.

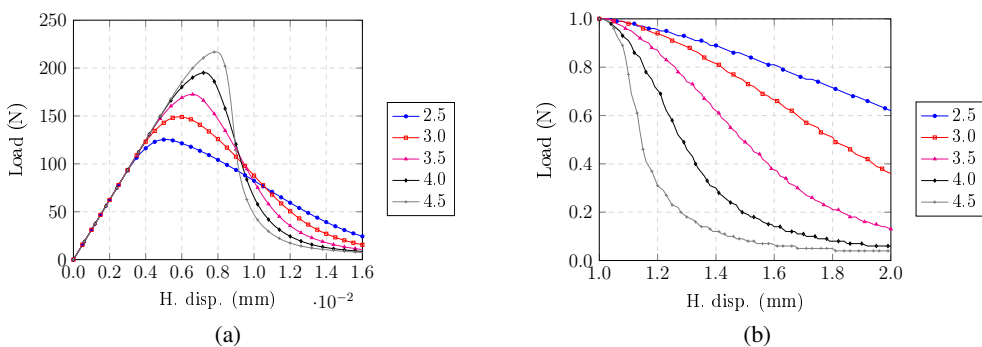


Figure 7. Load-displacement curves for various tensile strength ( $f_t$ ) parameters. The unit of the therms shown in legend is  $N/mm^2$ . (a) Load-displacement curve. (b) Normalized load-displacement curve.

It can be noted that the structure is more ductile for lower mortar tensile strengths in such way that, for  $f_t = 4.5 N/mm^2$ , the softening is almost vertical. Such behavior is coherent since, as the fracture energy is the same for all tests, the area under the curve corresponding to the softening must be kept unchanged.

From Fig. 7, it is worth to note that for the realized tests, there is a point in the softening branch very close to all curves.

## 4 Aggregate Properties

The tests presented in this section are similar to that of section 3, but now varying the parameters of the aggregates. Again, it will be considered the sample of 50 mm, modelled as a plane stress state with the Phase-Field Isotropic constitutive model. The properties presented in section 2 were used.

### 4.1 Different Fracture Energy and Tensile Strength Parameters

The variation of the fracture energy ( $G_f$ ) and the tensile strength ( $f_t$ ) were considered in here. Fig. 8.a shows the load-displacement curves varying the fracture energy, and Fig. 8.b varying the elasticity modulus. The units of the numerical values presented in the legend are N/mm for the fracture energy and N/mm<sup>2</sup> for the tensile strength.

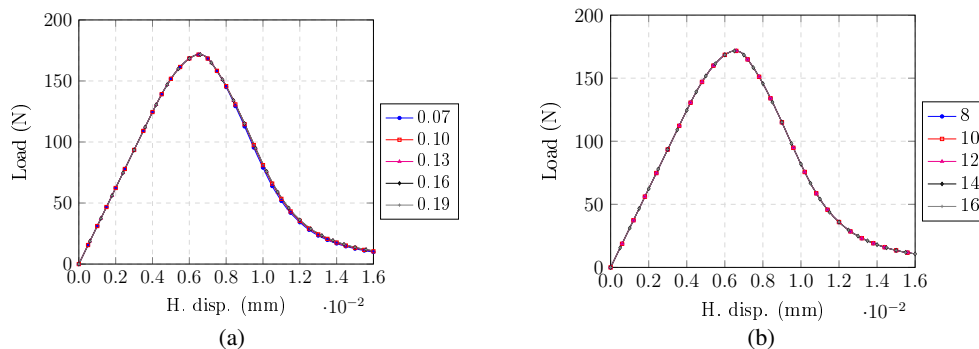


Figure 8. Load-displacement curves for varying the parameters of the aggregate. (a) Varying the fracture energy ( $G_f$ ). The unit of the term shown in legend is N/mm. (b) Varying the tensile strength ( $f_t$ ). The unit of the term shown in legend is N/mm<sup>2</sup>.

As it can be seen, the behaviour hasn't changed by varying the proprieties. This feature can be understood observing the phase-field contour plots presented in Fig. 4. As the aggregate is much more resistant than the mortar, the Phase-Field parameter in that continues equal to zero and its behaviour remains linear elastic. In this way, the structural response in terms of non-linearity is strictly controlled by the mortar.

### 4.2 Different Elasticity Modulus

In this last subsection, it is presented the behaviour of the sample considering various elasticity modulus for the aggregate. The graphs shown in Fig. 9 presents the load-displacement and the normalized load-displacement

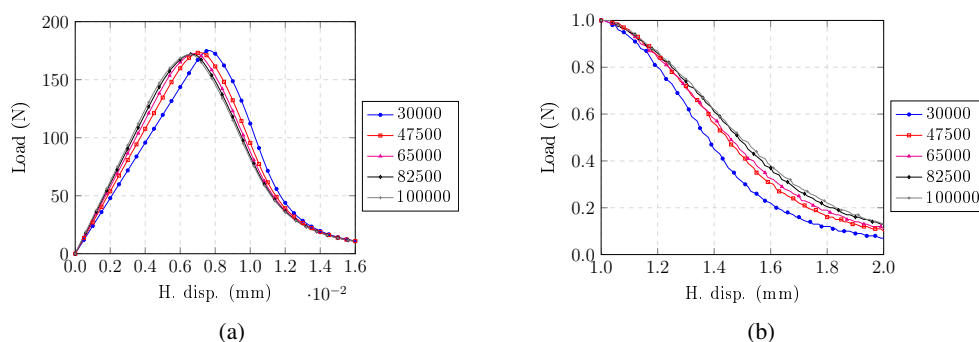


Figure 9. Load-displacement curve for various elasticity modulus ( $E_0$ ) parameters. The unit of the terms shown in legend is N/mm<sup>2</sup>. (a) Load-displacement curve. (b) Normalized load-displacement curve.

curves. The numerical values presented in the legend are defined in N/mm<sup>2</sup>. The results shows that a greater elasticity modulus for the aggregate provides more ductility and stiffness to the structure (See Fig. 9).b. Although

that variation is observed, the difference between the curves is not representative when comparing with the results presented in section 2. In other words, the behaviour of the considered concrete specimen was mainly driven by the mortar properties.

## 5 Conclusions

The main purpose of this article was to study the behaviour of a heterogeneous material under a traction test, using the Phase-Field model implemented in INSANE. For that, the Phase-Field isotropic constitutive model with the linear energetic degradation function and the geometric crack function of Wu [14] with parameter  $\xi = 2$  was considered. To place the aggregates randomly in the domain, the *Take and Place* method was used [12, 13]. In section 2, the mortar and aggregate parameters were fixed, and the size of sample was varied. The results have shown that the big samples provides a very fragile response. For test using the model with 100 mm of size (Fig. 2.f) the softening branch was vertical. Sections 3.1 and 4.1 have analysed the structural behaviour by varying the properties of the mortar and the aggregate. From the presented results, it can be concluded that the variation of aggregate properties has a small effect on the structural behaviour. That is because the crack have happened only in mortar and, therefore, the strains in the aggregate remains in the linear elastic part of the stress-strain curve. In other words, in the realized tests, the structural behaviour were mainly controlled by the mortar properties. In this way, analysing only the mortar parameters, it was found that the variation in fracture energy ( $G_f$ ) affects structure fragility, where the specimens with lower values are more fragile. As for the variation in elasticity modulus ( $E_0$ ), it changes satisfactorily the initial linear elastic branch and, in terms of structural fragility, it could be seen that the increasing of that parameter makes the structure more ductile. And finally, when comparing different mortar tensile strengths, it can be noted that, higher values promotes a more stronger structure, but much more fragile.

**Acknowledgements.** The authors gratefully acknowledge the support from the Brazilian research agencies CAPES (*Coordenação de Aperfeiçoamento de Pessoal de Nível Superior*), FAPEMIG (*Fundação de Amparo à Pesquisa do Estado de Minas Gerais*; Grant PPM-00747-18) and CNPq (*Conselho Nacional de Desenvolvimento Científico e Tecnológico*; Grant 316240/2021-4).

**Authorship statement.** The authors hereby confirm that they are the sole liable persons responsible for the authorship of this work, and that all material that has been herein included as part of the present paper is either the property (and authorship) of the authors, or has the permission of the owners to be included here.

## References

- [1] D. J. Carreira and K.-H. Chu. Stress-strain relationship for plain concrete in tension. *American Concrete Institute Journal*, vol. 83 (1), pp. 21–28, 1986.
- [2] I. Carol, P. C. Prat, and Z. P. Bažant. New explicit microplane model for concrete: Theoretical aspects and numerical implementation. *International Journal of Solids and Structures*, vol. 29, n. 9, pp. 1173–1191, 1992.
- [3] R. L. d. S. Pitangueira. *Mecânica de estruturas de concreto com inclusão de efeitos de tamanho e heterogeneidade*. Phd thesis, Pontifícia Universidade Católica do Rio de Janeiro. (in portuguese), 1998.
- [4] R. Borst and M. A. Gutiérrez. A unified framework for concrete damage and fracture models including size effects. *International Journal of Fracture*, vol. 95, pp. 261–277, 1999.
- [5] K. P. Wolf. Implementação computacional de um modelo de fissuração para o concreto baseado no método dos elementos finitos estendido (xfem). Master dissertation, Universidade Federal de Minas Gerais (UFMG). (in portuguese), 2010.
- [6] S. S. Pena, R. L. d. S. Pitangueira, and J. S. Fuina. Comparative study of smeared cracking models for concrete structures. *Semina: Ciências Exatas e Tecnológicas*, vol. 34, 2013.
- [7] A phase field method to simulate crack nucleation and propagation in strongly heterogeneous materials from direct imaging of their microstructure. *Engineering Fracture Mechanics*, vol. 139, pp. 18–39, 2015.
- [8] J.-Y. Wu, V. P. Nguyen, C. Thanh Nguyen, D. Sutula, S. Bordas, and S. Sinaie. Chapter One - Phase-field modeling of fracture. *Advances in Applied Mechanics*, vol. 53, pp. 1–183, 2020.
- [9] A. C. Hansen-Dörr, F. Dammaß, R. de Borst, and M. Kästner. Phase-field modeling of crack branching and deflection in heterogeneous media. *Engineering Fracture Mechanics*, vol. 232, pp. 107004, 2020.
- [10] X. Hu, X. Gong, N. Xie, Q. Zhu, P. Guo, H. Hu, and J. Ma. Modeling crack propagation in heterogeneous granite using grain-based phase field method. *Theoretical and Applied Fracture Mechanics*, vol. 117, pp. 103203, 2022.

- [11] B. Bourdin, G. Francfort, and J.-J. Marigo. The variational approach to fracture. *Reprinted from J. Elasticity*, vol. 91, pp. 5–148, 2008.
- [12] Z. Wang, A. Kwan, and H. Chan. Mesoscopic study of concrete i: generation of random aggregate structure and finite element mesh. *Computers and Structures*, vol. 70, n. 5, pp. 533–544, 1999.
- [13] P. Wriggers and S. Moftah. Mesoscale models for concrete: Homogenisation and damage behaviour. *Finite Elements in Analysis and Design*, vol. 42, n. 7, pp. 623–636. The Seventeenth Annual Robert J. Melosh Competition, 2006.
- [14] J.-Y. Wu. A unified phase-field theory for the mechanics of damage and quasi-brittle failure. *Journal of the Mechanics and Physics of Solids*, vol. 103, pp. 72–99, 2017.